A Graph-Embedded Latent Space Learning and Clustering Framework for Incomplete Multimodal Multiclass Alzheimer's Disease Diagnosis

Zaixin Ou[1], Caiwen Jiang[1], Yuxiao Liu[1], Yuanwang Zhang[1], Zhiming Cui[1], and Dinggang Shen[1,2,3]

[1] School of Biomedical Engineering & State Key Laboratory of Advanced Medical Materials and Devices, ShanghaiTech University, Shanghai 201210, China
[2] Shanghai United Imaging Intelligence Co., Ltd., Shanghai 200232, China
[3] Shanghai Clinical Research and Trial Center, Shanghai 201210, China
dgshen@shanghaitech.edu.cn

Abstract. Alzheimer's disease (AD) is an irreversible neurodegenerative disease, where early diagnosis is crucial for improving prognosis and delaying the progression of the disease. Leveraging multimodal PET images, which can reflect various biomarkers like Aβ and tau protein, is a promising method for AD diagnosis. However, due to the high cost and practical issues of PET imaging, it often faces challenges with incomplete multimodal data. To address this dilemma, in this paper, we propose a **Graph**-embedded latent **S**pace **L**earning and **C**lustering framework, named **Graph-SLC**, for multiclass AD diagnosis under incomplete multimodal data scenarios. The key concept is leveraging all available subjects, including those with incomplete modality data, to train **a network** for projecting subjects into their latent representations. These latent representations *not only* exploit the complementarity of different modalities *but also* showcase separability among different classes. Specifically, our Graph-SLC consists of three modules, i.e., a multimodal reconstruction module, a subject-similarity graph embedding module, and an AD-oriented latent clustering module. Among them, the multimodal reconstruction module generates subject-specific latent representations that can comprehensively incorporate information from different modalities with guidance from all available modalities. The subject-similarity graph embedding module then enhances the discriminability of different latent representations by ensuring the neighborhood relationships between subjects are preserved in subject-specific latent representations. The AD-oriented latent clustering module facilitates the separability of multiple classes by constraining subject-specific latent representations within the same class to be in the same cluster. Experiments on the ADNI show that our method achieves state-of-the-art performance in multiclass AD diagnosis. Our code is available at https://github.com/Ouzaixin/Graph-SLC.

Keywords: Alzheimer's Disease · Incomplete Multimodal Learning · Graph Embedding · Latent Space Clustering.

1 Introduction

Alzheimer's disease (AD) is a neurodegenerative disorder that causes symptoms, such as memory loss, language difficulties, and disorientation, posing a significant threat to patients' health [3, 18]. Despite substantial resources have been devoted, there are currently no effective treatments to cure AD. In this context, early diagnosis of AD is crucial for timely interventions that may prevent or at least delay the progress of AD, as well as its prodrome, i.e., mild cognitive impairment (MCI) [15, 16]. Among various diagnostic approaches, multimodal PET diagnosis stands out as the most promising method due to its capability to reflect changes in multiple AD-related biomarkers. However, due to the high radiation risk and cost associated with PET imaging, this approach often faces challenges with incomplete multimodal data [1, 21].

There have been some studies attempting to address the issue of missing data in multimodal PET diagnosis. These studies can be categorized into two categories: missing data imputation [14, 17, 25] and latent space learning [27, 28, 13, 7]. The missing data imputation-based methods aim to complete missing data through generative models. For example, Pan *et al.* [14] proposed a feature-consistency generative adversarial network to impute missing PET images from MRI, and then utilize the completed data for AD diagnosis. However, such methods typically require a large number of subjects with paired data to train the generation network, while paired data are often limited and difficult to obtain. Moreover, the process of generating missing data may introduce redundant or biased information, potentially affecting the final diagnosis [4].

To overcome these limitations, some studies [23, 12, 11, 9] have focused on developing latent space learning-based methods to flexibly handle incomplete multimodal data without requiring imputation of missing data. Compared to imputation-based methods, latent space learning-based methods project input data into the lower-dimensional latent to extract essential information. Besides, latent space learning-based methods can flexibly handle incomplete multimodal data scenarios in practical applications without the necessity of paired data. For example, Zhou *et al.* [27] utilize all available subjects (including subjects with incomplete modality data) to learn a latent space, and then project the latent space to the label space for AD diagnosis. However, such methods treat the latent space as two separate components: a modality-common latent space and a modality-specific latent space, failing to fully leverage the complementary information between different modalities, which results in suboptimal performance [10]. Besides, they overlook relationships between the latent representations of different subjects, making it challenging to derive discriminative latent representations [22].

Instead of dividing the latent space into separate parts, our method proposes to learn a whole comprehensive latent representation for each subject. This subject-specific latent representation *not only* explores the complementary information of different modalities *but also* demonstrates separability among different classes. To achieve this, in this paper, we propose a graph-embedded latent space learning and clustering framework for incomplete multimodal multiclass

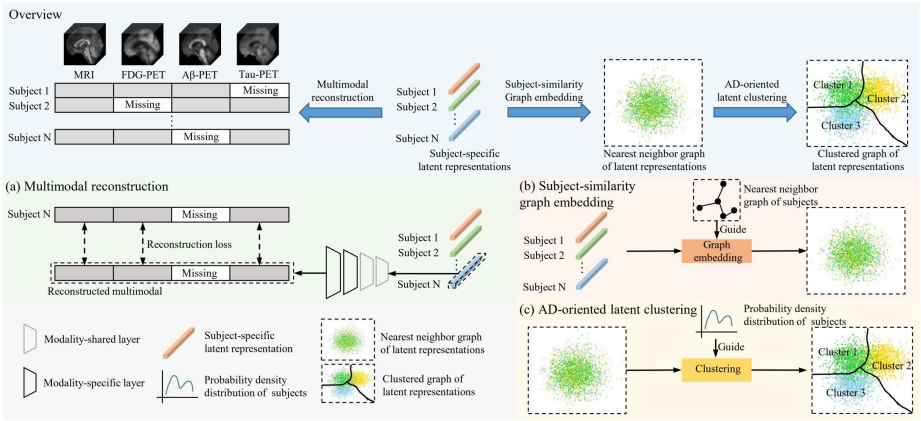

Fig. 1. Illustration of our proposed Graph-SLC. It consists of three modules: a) A multimodal reconstruction module to generate the subject-specific latent representations that can comprehensively incorporate information from different modalities with guidance from all available modalities; b) A subject-similarity graph embedding module to constrain the latent representations to preserve neighborhood relationships within subjects; c) An AD-oriented latent clustering module to improve the separability of the latent representations across different disease classes.

AD diagnosis. First, we utilize a multimodal reconstruction module to generate subject-specific latent representations that can comprehensively incorporate information from different available modalities. Second, to enhance the discriminability of different latent representations, we introduce a subject-similarity graph embedding module to ensure that the neighborhood relationships between subjects are maintained in latent representations. Third, to facilitate the separability of multiple classes, we introduce an AD-oriented latent clustering module to constrain latent representations of the same class to be clustered together.

The main contributions of our work include: i) Proposing a graph-embedded latent space learning and clustering framework for incomplete multimodal multi-class AD diagnosis, with the capability of handling incomplete multimodal data scenarios; ii) Employing a subject-similarity graph embedding module to ensure integrity of neighborhood relationships within the latent space, thereby deriving discriminative latent representations effectively; iii) Introducing an AD-oriented latent clustering module to enhance separability of multiple classes within the latent space for capturing the characteristics of class distributions among subjects.

2 Method

Our proposed Graph-SLC is illustrated in Fig. 1, comprising three key components, including 1) multimodal reconstruction module, 2) subject-similarity graph embedding module, and 3) AD-oriented latent clustering module. For a

given subject, the multimodal reconstruction module first generates a subject-specific latent representation, which integrates information from different modalities under the guidance of all available modalities. Subsequently, the latent representation is constrained by the subject-similarity graph embedding module to maintain neighborhood relationships between the input subject and other subjects within the latent space. Finally, the latent representation is fed into the AD-oriented latent clustering module to enhance its separability across different disease categories. We introduce details of each component in our Graph-SLC below.

2.1 Multimodal Reconstruction

Recent studies have demonstrated that multimodal data can improve performance of multiclass AD diagnosis by providing complementary information [14, 29, 19]. Thus, to capture complementary information between different modalities, we project subjects with arbitrary modality-missing patterns into the corresponding latent representations, each of which incorporates information from different modalities. For example, given a subject s_i in the dataset $\mathbf{S}$ with M partial modalities $\{x_i^1, \ldots, x_i^M\}$, we can model the likelihood of the subject-specific latent representation z_i as:

$$p(s_i|z_i) \propto e^{-\mathcal{L}_r(s_i, f_r(z_i))} \tag{1}$$

where $p(s_i|z_i) = p(x_i^1|z_i)p(x_i^2|z_i)\ldots p(x_i^M|z_i)$, which assumes that each modality can be reconstructed from a complete representation in a numerically stable way [24]. $\mathcal{L}_r(s_i, f(z_i))$ is the multimodal reconstruction loss, which can be formulated as:

$$\mathcal{L}_r = \sum_{i=1}^{N}\sum_{j=1}^{M} ||x_i^j - f(z_i)||_2^2 \tag{2}$$

where $f(\cdot)$ represents the reconstruction mapping from the latent representation z_i to M partial modalities of subject s_i. We construct $f(\cdot)$ using four layers of upsampling and residual blocks. Specifically, the first two layers are shared among all modalities, while the latter two layers are modality-specific, as illustrated in Fig. 1(a).

2.2 Subject-similarity Graph Embedding

In the field of latent space learning, a recognized manifold assumption is that if two data points are close to each other, their corresponding low-dimensional representations should be also close in the latent space [20]. Drawing inspiration from this principle, we extend this concept to the relationships between subjects. For example, considering two subjects $s_i = [x_i^1, x_i^2]$ and $s_j = [x_j^1, \emptyset]$, if these two subjects are very similar, their latent representations either by complete modalities (i.e., z_i) or by incomplete modalities (i.e., z_j) should also maintain such neighborhood relationships. Consequently, by pulling the corresponding latent

representations of these two subjects closer in the latent space, the latent representation of s_j can implicitly capture information about missing modality x_j^2, thereby enhancing diagnostic capacity of this latent representation. To preserve the integrity of such neighborhood relationships within the latent space, we introduce a graph embedding loss:

$$\mathcal{L}_g = \frac{1}{2N} \sum_{i=1}^{n} \sum_{j=1}^{n} \|z_i - z_j\|_2^2 G_{ij} \tag{3}$$

where G_{ij} denotes the nearest neighbor graph constructed from subjects $\mathbf{S}$ as follows:

$$G_{ij} = \begin{cases} 1, & \text{if } (\psi(s_i) \in s_j \text{ or } \psi(s_j) \in s_i) \\ 0, & \text{otherwise} \end{cases} \tag{4}$$

where $\psi(s_i)$ denotes the nearest subject to s_i. To determine $\psi(s_i)$, we identify the subject with the lowest average difference between the modalities shared by s_i and those of the remaining subjects.

2.3 AD-oriented Latent Clustering

AD is a progressive disease, with no significant difference between various stages (especially between MCI and AD), posing significant challenge for multiclass AD diagnosis. To address this challenge, we design a targeted AD-oriented latent clustering algorithm to enhance the separability across different classes in the latent space. Specifically, we first utilize a spectral clustering algorithm [8] on the latent representations to perform latent space clustering. Subsequently, based on the clustering result, we compute probability density distributions of the latent representations. Finally, we introduce a distribution consistency loss [26] to minimize discrepancy between the probability density distributions of latent representations and the probability density distributions of subjects, as depicted in Fig. 1(c). The distribution consistency loss can be expressed as follows:

$$\mathcal{L}_d = \sum_{i=1}^{N} \hat{f}(s_i) log \frac{\hat{f}(s_i)}{\hat{f}(z_i)} \tag{5}$$

where $\hat{f}(s_i)$ and $\hat{f}(z_i)$ are the probability density distribution of subjects $\mathbf{S} = [s_i, \ldots, s_N]$ and their corresponding latent representations $\mathbf{Z} = [z_i, \ldots, z_N]$, respectively. We use kernel density estimation [2], a nonparametric technique, to estimate the probability density distribution.

Based on the above considerations, the overall objective function is induced as:

$$\mathcal{L} = \mathcal{L}_r + \lambda_1 \mathcal{L}_g + \lambda_2 \mathcal{L}_d \tag{6}$$

where $\mathcal{L}_r$ represents the multimodal reconstruction loss, $\mathcal{L}_g$ denotes the graph embedding loss, and $\mathcal{L}_d$ is the distribution consistency loss. Additionally, λ_1 and λ_2 are the two weighting factors for the $\mathcal{L}_g$ and $\mathcal{L}_d$ loss terms, respectively.

Table 1. Demographics for the dataset, with some data shown as mean±std.

	AD (410)	MCI (1080)	CN (868)
Gender (Female/Male)	180/230	450/630	486/382
APOE (ε4/non ε4)	262/148	503/577	243/625
Age	74.94±7.77	72.83±7.64	72.50±6.60
MMSE	23.17±2.22	27.61±1.86	29.08±1.11
Years of education	15.23±2.91	15.98±2.76	16.52±2.53

3 Experiments

3.1 Materials and Experimental Setup

To validate our proposed Graph-SLC, we collected 2358 subjects from the public Alzheimer's Disease Neuroimaging Initiative (ADNI) dataset[4]. Of these 2358 subjects, 1416 subjects are used for training, 471 for validation, and other 471 for testing. All subject have MRI scans, but only some of them have additional multimodal PET scans available, including FDG-PET, Aβ-PET, and Tau-PET. Further details about the collected dataset are provided in Table 1. All T1-weighted MRI scans underwent preprocessing via a standard pipeline, which included intensity correction, skull-stripping, and linear alignment to the Montréal Neurological Institute (MNI) template. Each PET scan was aligned with its corresponding MRI scan and registered to the template using the same affine matrix as its corresponding MRI scan. To eliminate anisotropy, all images were resampled to dimensions of $192 \times 192 \times 192$ with a voxel spacing of 1 mm^3.

In our implementation, the learning rate is set to $1e^{-4}$, and the weight decay is set to $5e^{-5}$. We assign weights λ_1 and λ_2 in the loss function as 1 and 0.1, respectively. All models in this study are trained for 40 epochs and are subject to early stopping if the loss does not decrease for 20 consecutive epochs. We train the models using PyTorch on a single NVIDIA Tesla A100 GPU. Evaluation is performed using five-fold cross-validation. Across all experiments, we assess performance based on diagnosis accuracy (ACC), precision (PRE), specificity (SPE), and F1-Score (F1S).

3.2 Performance of Proposed Method

To fully evaluate our proposed Graph-SLC, we explore its performance in multiclass AD diagnosis under different combinations of input modality data, with results provided in Table 2. The 1st to 4th rows in the table show the results under single modality. It can be observed that using Tau-PET for AD diagnosis achieves the best performance, followed by FDG-PET and MRI. Furthermore, the diagnostic performance using multiple modalities (5th to 7th rows) significantly surpasses that of using a single modality (1st to 4th). This demonstrates that our proposed Graph-SLC can effectively extract and utilize complementary

[4] https://adni.loni.usc.edu/

Table 2. The diagnostic performance of our Graph-SLC under different combinations of input modality data. Results are listed as mean ± std through five-fold cross-validation.

Different settings	ACC (%)↑	PRE (%)↑	SPE (%)↑	F1S (%)↑
Only MRI	57.00±1.45	57.47±1.31	55.15±1.49	56.82±1.45
Only FDG-PET	59.01±1.96	60.48±2.64	55.26±4.65	58.05±2.34
Only Aβ-PET	54.18±1.81	56.48±1.82	54.28±3.89	53.58±1.46
Only Tau-PET	62.03±2.36	62.04±2.69	51.59±2.65	57.16±2.34
w/o FDG-PET	64.47±1.77	65.28±1.55	64.36±1.92	**65.52±1.77**
w/o Aβ-PET	65.07±3.62	65.31±4.04	63.54±4.20	58.00±5.58
w/o Tau-PET	63.23±1.52	64.30±1.44	65.12±1.76	63.08±1.54
Ours	**65.18±1.35**	**65.83±1.53**	**65.23±1.33**	65.27±1.83

information from different modalities for diagnosis, thereby improving diagnostic performance.

3.3 Comparison with Other Methods

To further assess effectiveness of our proposed Graph-SLC, we further compare it with six state-of-the-art methods, which can be divided into two classes: 1) Data imputation methods, including Gao *et al.* [6], Pan *et al.* [14], and Wang *et al.* [19]; and 2) Latent space learning methods, including Zhou *et al.* [27], Ning *et al.* [13], Chen *et al.* [5]. All methods use the same experimental settings, and their quantitative results are given in Table 3.

From Table 3, it can be observed that our Graph-SLC achieved the best performance among all the methods, with 2.14%, 1.48%, 1.89%, and 3.03% improvements in ACC, PRE, SPE, and F1S, respectively, compared to the sub-optimal method (Chen *et al.* [5]). This finding strongly validates effectiveness of our proposed Graph-SLC. Furthermore, our analysis reveals that, on average, imputation-based methods perform inferiorly compared to the latent space learning methods. This could be attributed to introduction of excessive redundant and biased information in the synthesized PET images by imputation-based methods, thereby leading to poor classification results. In contrast, latent space learning-based methods can achieve good performance, as they effectively mitigate generation of redundant information by acquiring a low-dimensional representation of a high-dimensional space. This allows for extracting more meaningful and discriminative features, leading to improved classification performance.

3.4 Ablation Study

We design relevant ablation experiments to analyze effectiveness of the two proposed key modules, including 1) subject-similarity graph embedding and 2) AD-oriented latent clustering. The experimental results under different combinations of these two modules are provided in Table 4. As shown in the table, the integration of subject-similarity graph embedding and AD-oriented latent clustering significantly enhances the model's performance, outperforming the scenarios

Table 3. Quantitative comparison of our Graph-SLC with several state-of-the-art methods. Results are shown as mean±std through five-fold cross-validation.

Method		ACC (%)↑	PRE (%)↑	SPE (%)↑	F1S (%)↑
Missing data imputation	Gao *et al.* [6]	58.63±4.43	59.50±2.52	56.43±4.67	55.32±7.74
	Pan *et al.* [14]	59.44±4.01	60.54±3.50	54.64±3.88	58.87±3.99
	Wang *et al.* [19]	62.02±2.29	64.15±2.84	62.71±2.44	61.71±2.54
Latent space learning	Zhou *et al.* [27]	60.33±1.85	60.87±1.06	58.26±3.47	60.01±1.34
	Ning *et al.* [13]	61.50±1.88	63.38±1.54	63.48±2.09	60.35±1.87
	Chen *et al.* [5]	63.04±2.47	64.35±2.86	63.34±2.54	62.24±2.72
	Ours	**65.18±1.35**	**65.83±1.53**	**65.23±1.33**	**65.27±1.83**

Table 4. Quantitative results of ablation study. Results are listed as mean±std across the test set.

Method	ACC (%)↑	PRE (%)↑	SPE (%)↑	F1S (%)↑
Ours (w/o embedding, clustering)	61.88±2.91	64.31±3.68	63.40±3.18	60.80±3.64
Ours (w/o embedding)	64.43±2.67	65.67±3.30	**65.53±1.34**	64.19±2.79
Ours (w/o clustering)	62.38±2.70	64.87±3.30	63.00±3.31	61.28±3.55
Ours	**65.18±1.35**	**65.83±1.53**	65.23±1.33	**65.27±1.83**

without these modules. The incorporation of subject-similarity graph embedding ensures the latent representation maintains neighborhood relationships during the learning process, retaining local structural information within the original space. Simultaneously, the introduction of AD-oriented latent clustering enables the model to understand the characteristics of class distribution among subjects, resulting in more accurate clustering. Experimental results demonstrate that removing either module degrades the model's performance, further indicating importance of these two key strategies. In summary, the combination of subject-similarity graph embedding and AD-oriented latent clustering plays a crucial role in improving model performance, offering an effective approach for multiclass diagnosis tasks.

4 Conclusions

To address the missing data problem in the joint diagnosis of AD when using multimodal PET, we propose a graph-embedded latent space learning and clustering framework. Specifically, we first use a multimodal reconstruction module to generate subject-specific latent representations that can comprehensively incorporate information from different available modalities. Then, a subject-similarity graph embedding module is used to constrain subject-specific latent representations to preserve the neighborhood relationships within subjects. Finally, we employ an AD-oriented latent clustering module to force latent representations of the same class to be in the same cluster. Experiments on an ADNI dataset with 2358 subjects show that our proposed model achieves state-of-the-art performance in multiclass AD diagnosis, suggesting effectiveness of our proposed model in tackling modality-missing issue.

Acknowledgments. This work was supported in part by National Natural Science Foundation of China (grant numbers 62131015, 62250710165, U23A20295), the STI 2030-Major Projects (No. 2022ZD0209000), Shanghai Municipal Central Guided Local Science and Technology Development Fund (grant number YDZX20233100001001), Science and Technology Commission of Shanghai Municipality (STCSM) (grant number 21010502600), and The Key R&D Program of Guangdong Province, China (grant numbers 2023B0303040001, 2021B0101420006).

Disclosure of Interests. The authors declare that they have no conflict of interest.

References

1. Azad, R., Khosravi, N., Dehghanmanshadi, M., Cohen-Adad, J., Merhof, D.: Medical image segmentation on MRI images with missing modalities: A review. arXiv preprint arXiv:2203.06217 (2022)
2. Bailey, T.C., Gatrell, A.C., et al.: Interactive spatial data analysis, vol. 413. Longman Scientific & Technical Essex (1995)
3. Baumgart, M., Snyder, H.M., Carrillo, M.C., Fazio, S., Kim, H., Johns, H.: Summary of the evidence on modifiable risk factors for cognitive decline and dementia: a population-based perspective. Alzheimer's & Dementia **11**(6), 718–726 (2015)
4. Chen, Y., Pan, Y., Xia, Y., Yuan, Y.: Disentangle first, then distill: A unified framework for missing modality imputation and Alzheimer's disease diagnosis. IEEE Transactions on Medical Imaging (2023)
5. Chen, Z., Liu, Y., Zhang, Y., Li, Q., Initiative, A.D.N., et al.: Orthogonal latent space learning with feature weighting and graph learning for multimodal Alzheimer's disease diagnosis. Medical Image Analysis **84**, 102698 (2023)
6. Gao, X., Shi, F., Shen, D., Liu, M.: Task-induced pyramid and attention GAN for multimodal brain image imputation and classification in Alzheimer's disease. IEEE journal of biomedical and health informatics **26**(1), 36–43 (2021)
7. Guan, Y., Li, Y., Liu, R., Meng, Z., Li, Y., Ying, L., Du, Y.P., Liang, Z.P.: Subspace model-assisted deep learning for improved image reconstruction. IEEE transactions on medical imaging (2023)
8. Kang, Z., Shi, G., Huang, S., Chen, W., Pu, X., Zhou, J.T., Xu, Z.: Multi-graph fusion for multi-view spectral clustering. Knowledge-Based Systems **189**, 105102 (2020)
9. Li, A., Feng, C., Cheng, Y., Zhang, Y., Yang, H.: Incomplete multiview subspace clustering based on multiple kernel low-redundant representation learning. Information Fusion **103**, 102086 (2024)
10. Li, R., Zhang, C., Fu, H., Peng, X., Zhou, T., Hu, Q.: Reciprocal multi-layer subspace learning for multi-view clustering. In: Proceedings of the IEEE/CVF international conference on computer vision. pp. 8172–8180 (2019)
11. Liu, J., Liu, X., Zhang, Y., Zhang, P., Tu, W., Wang, S., Zhou, S., Liang, W., Wang, S., Yang, Y.: Self-representation subspace clustering for incomplete multiview data. In: Proceedings of the 29th ACM international conference on multimedia. pp. 2726–2734 (2021)
12. Liu, M., Zhang, J., Yap, P.T., Shen, D.: View-aligned hypergraph learning for Alzheimer's disease diagnosis with incomplete multi-modality data. Medical image analysis **36**, 123–134 (2017)

13. Ning, Z., Xiao, Q., Feng, Q., Chen, W., Zhang, Y.: Relation-induced multi-modal shared representation learning for Alzheimer's disease diagnosis. IEEE Transactions on Medical Imaging **40**(6), 1632–1645 (2021)
14. Pan, Y., Liu, M., Xia, Y., Shen, D.: Disease-image-specific learning for diagnosis-oriented neuroimage synthesis with incomplete multi-modality data. IEEE transactions on pattern analysis and machine intelligence **44**(10), 6839–6853 (2021)
15. Reiman, E.M., Langbaum, J.B., Tariot, P.N.: Alzheimer's prevention initiative: a proposal to evaluate presymptomatic treatments as quickly as possible. Biomarkers in medicine **4**(1), 3–14 (2010)
16. Ruan, D., Sun, L.: Amyloid-β PET in Alzheimer's disease: A systematic review and bayesian meta-analysis. Brain and Behavior **13**(1), e2850 (2023)
17. Sikka, A., Virk, J.S., Bathula, D.R., et al.: MRI to PET cross-modality translation using globally and locally aware GAN (GLA-GAN) for multi-modal diagnosis of Alzheimer's disease. arXiv preprint arXiv:2108.02160 (2021)
18. Tarawneh, R., Holtzman, D.M.: The clinical problem of symptomatic Alzheimer disease and mild cognitive impairment. Cold Spring Harbor perspectives in medicine **2**(5) (2012)
19. Wang, C., Piao, S., Huang, Z., Gao, Q., Zhang, J., Li, Y., Shan, H., Initiative, A.D.N., et al.: Joint learning framework of cross-modal synthesis and diagnosis for Alzheimer's disease by mining underlying shared modality information. Medical Image Analysis **91**, 103032 (2024)
20. Wen, J., Zhang, Z., Xu, Y., Zhang, B., Fei, L., Xie, G.S.: Cdimc-net: Cognitive deep incomplete multi-view clustering network. In: Proceedings of the Twenty-Ninth International Conference on International Joint Conferences on Artificial Intelligence. pp. 3230–3236 (2021)
21. Xie, G., Huang, Y., Wang, J., Lyu, J., Zheng, F., Zheng, Y., Jin, Y.: Cross-modality neuroimage synthesis: A survey. ACM computing surveys **56**(3), 1–28 (2023)
22. Yan, W., Zhang, Y., Tang, C., Zhou, W., Lin, W.: Anchor-sharing and clusterwise contrastive network for multiview representation learning. IEEE Transactions on Neural Networks and Learning Systems (2024)
23. Yin, Q., Wu, S., Wang, L.: Unified subspace learning for incomplete and unlabeled multi-view data. Pattern Recognition **67**, 313–327 (2017)
24. Zhang, C., Han, Z., Fu, H., Zhou, J.T., Hu, Q., et al.: CPM-Nets: Cross partial multi-view networks. Advances in Neural Information Processing Systems **32** (2019)
25. Zhang, J., He, X., Qing, L., Gao, F., Wang, B.: Bpgan: Brain PET synthesis from MRI using generative adversarial network for multi-modal Alzheimer's disease diagnosis. Computer Methods and Programs in Biomedicine **217**, 106676 (2022)
26. Zhou, L., Xiao, B., Liu, X., Zhou, J., Hancock, E.R., et al.: Latent distribution preserving deep subspace clustering. In: 28th International joint conference on artificial intelligence. pp. 4440–4446. York (2019)
27. Zhou, T., Liu, M., Thung, K.H., Shen, D.: Latent representation learning for Alzheimer's disease diagnosis with incomplete multi-modality neuroimaging and genetic data. IEEE transactions on medical imaging **38**(10), 2411–2422 (2019)
28. Zhou, T., Canu, S., Vera, P., Ruan, S.: Latent correlation representation learning for brain tumor segmentation with missing mri modalities. IEEE Transactions on Image Processing **30**, 4263–4274 (2021)
29. Zhu, Q., Xu, B., Huang, J., Wang, H., Xu, R., Shao, W., Zhang, D.: Deep multi-modal discriminative and interpretability network for Alzheimer's disease diagnosis. IEEE Transactions on Medical Imaging (2022)